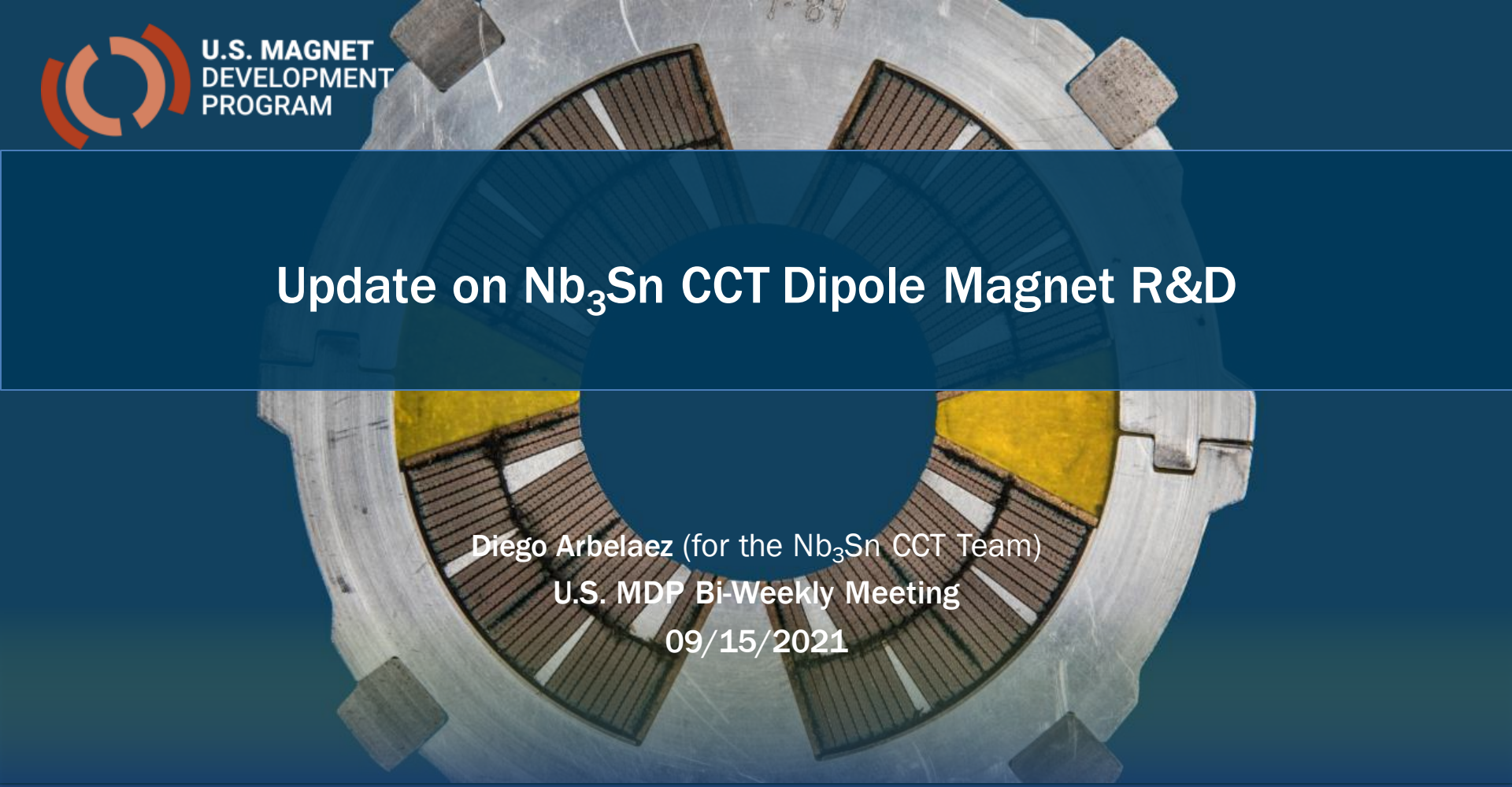

U.S. MAGNET DEVELOPMENT PROGRAM

Update on Nb_3Sn CCT Dipole Magnet R&D

Diego Arbelaez (for the Nb_3Sn CCT Team)

U.S. MDP Bi-Weekly Meeting

09/15/2021

Outline

- Subscale CCT magnets, test results, and planning
  - CCT subscale 2, 3, 4 magnet descriptions
  - Assembly process improvements
  - Magnet test results
  - Modeling of damage to interfaces
- Updates on CCT6 progress and planning
  - Modeling & Analysis
  - Machining of deep grooves

Subscale CCT Magnet Parameters

- 11 strand Nb3Sn cable
  - Strand diameters is 0.6 mm
  - Cable dimensions (1.1 x 4.0 mm)
  - 9100 A short sample current
  - Cable length ~ 50m
- Nominal inner bore diameter is 50 mm (thin spar)
- Bore dipole field is approximately 5.2 T as short sample current
- Peak conductor field is approximately 6.1 T at short sample current

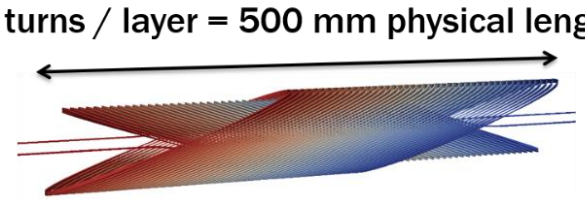

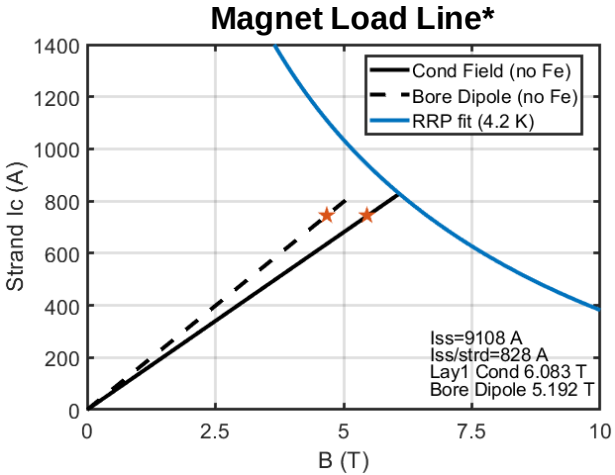

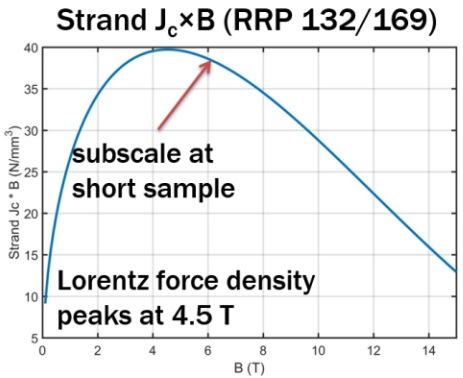

* Short sample measurements are based on similar wire used for superconducting undulators

Results of CCT SUB2 (Thin Spar / baseline) Demonstrate That Subscale CCTs Can Reasonably Reproduce Training Behavior Seen In Larger CCT Magnets

- Training slope for subscale (relative to SSL) is somewhat higher when compared with CCT5 but overall training behavior is similar
  - Reach 80% of SSL after 14 quenches in subscale
  - Reach 80% of SSL after 22 quenches in CCT5
- Thin spar subscale CCT has similar normal stress to CCT5 but lower shear stress
- Fast training segment is seen for first several quenches as was the case for CCT4

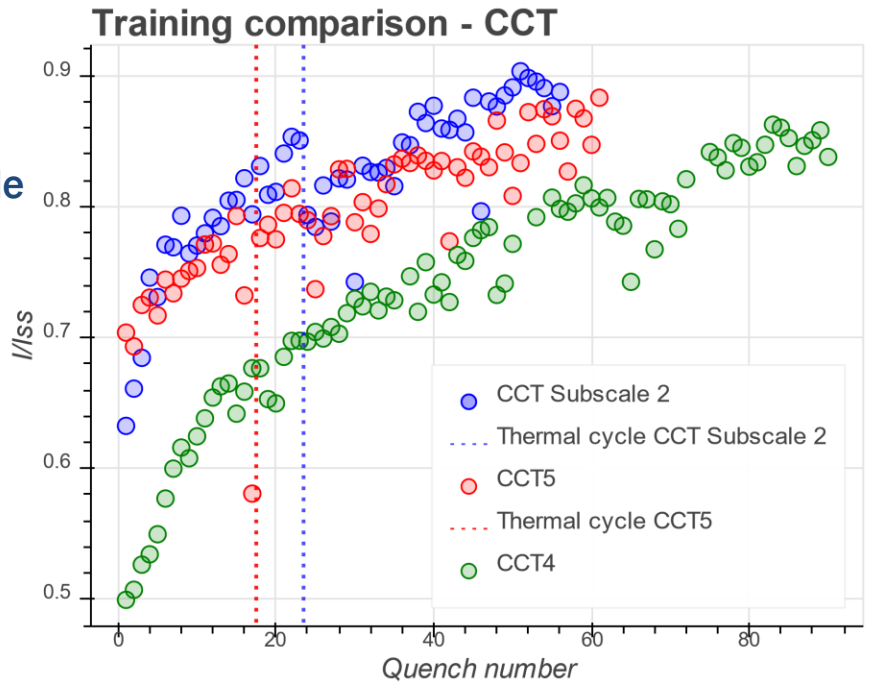

Fabrication Methods Are Similar To Those Used in CCT5

- Winding performed with light cable tension (by hand) as conductor is placed in groove
- Coils are wrapped in perforated stainless steel sheet for heat treatment
- Coil potting procedure is the same as for CCT5 (individual layer impregnation)
  - All potting materials are consumable except for end caps
  - FSU Mix 61 was used for impregnation CCT subscales 2 and 3, with new CTD resin used for subscale 4
  - Epoxy curing performed in an oven

Coil Winding with Vtap Flag

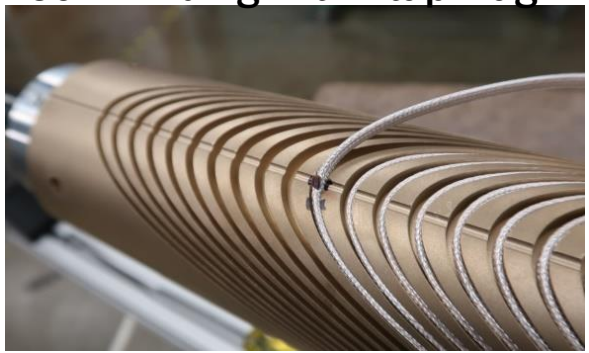

Potting Tooling

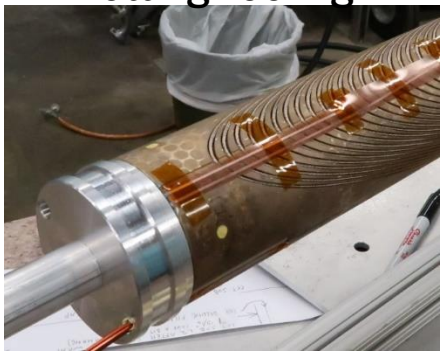

Potting Materials

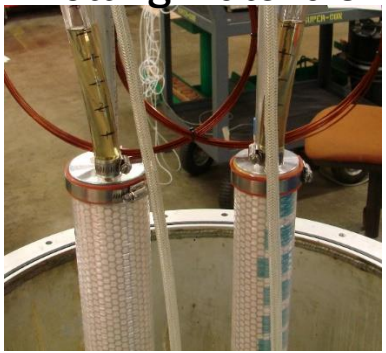

Impregnated Coil

First Two Subscale Magnets Focus on Understanding the Effect of Cable and Cable/Groove Interface Stress on Training

- Can use geometry of CCT coils to modify the stress in the cable and cable/groove interface
- Shear stress can be reduced by reducing spar thickness but normal stress will increase (accumulation of azimuthal force towards midplane + bending of layers)
- First set of tests is of inner layers with thin and thick spars
  - Thin spar → reduced interface shear stress and increased normal stress due to bending
  - Thick spar → increased interface shear stress and reduced normal stress due to bending

This spar is the baseline configuration which was chosen to replicate stress state in previous 2 layer models

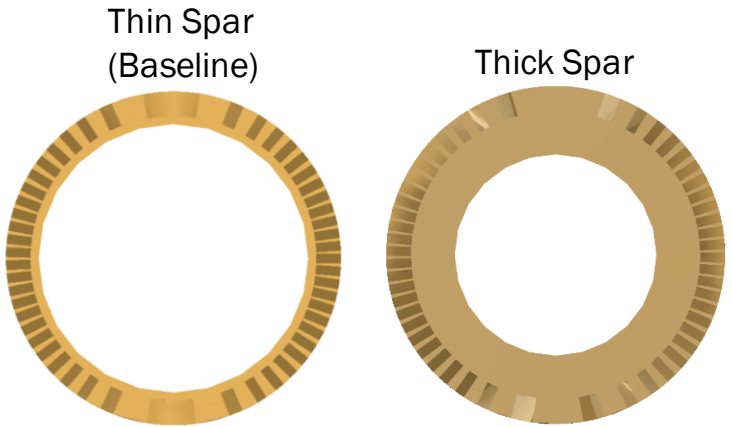

Third Subscale Magnet Focuses on Understanding the Effect of Impregnation Material on Training

- This magnet is part of SBIR with CTD to develop impregnation resins with improved properties for superconducting magnet applications (LBNL portion of effort led by T. Shen)
- Geometry is identical to CCT subscale 2 (thin spar / baseline)
- CTD 701x resin is used for impregnation of the inner and outer layer coils
  - Non-epoxy high toughness resin
- Some issues were encountered in the impregnation process for layer 2 due to outgassing – improvements were made for the second impregnation (layer 1)

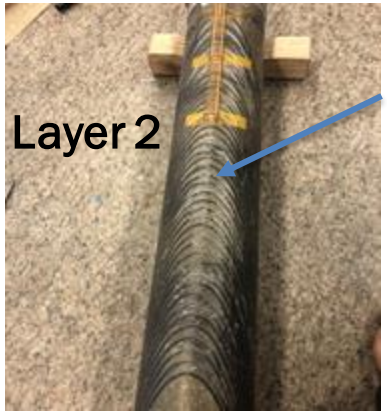

Gas bubbles are visible near pole region

Process was improved for layer 1 with less visible "bubbling"

Effort led by T. Shen, J. L. Rudeiros, J. Swanson, M. Krutulis

Assembly Method

- Contact location between layers is controlled by using shims and Kapton bags that are filled with glass and epoxy
  - Allows for control of contact location
  - Fracture in interface epoxy does not propagate to the coil
  - Improved cooling at the pole regions from direct contact with LHe
- Directional preload to reduce energized stress can be applied by bending layers or shell, filling and curing epoxy in bent state, releasing bending pressure

Layer 1,2 Assembly

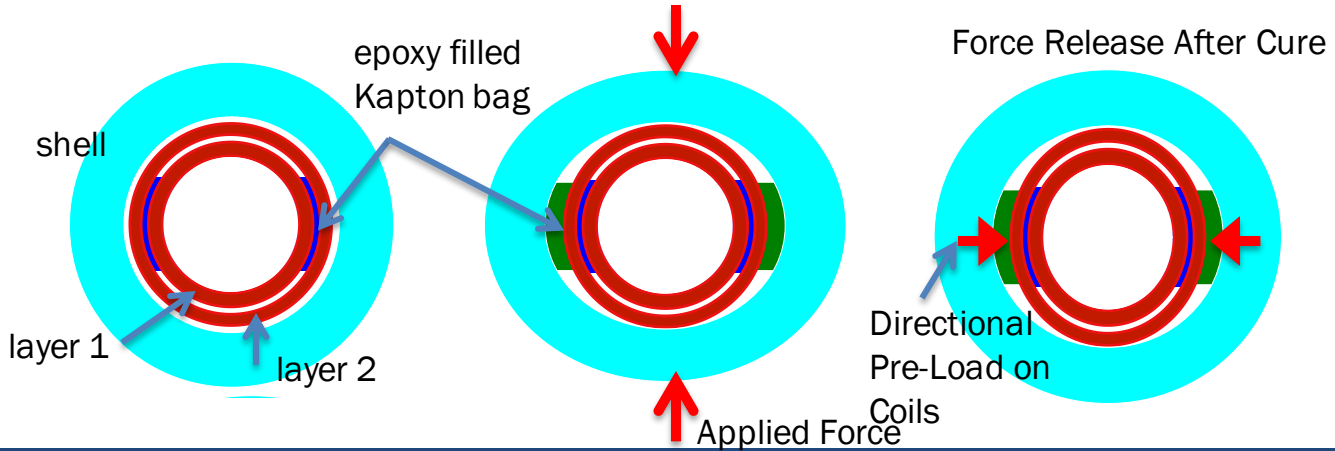

New methodology for the assembly of *smart* shims

- Improved process eliminates bubbles that were sometimes seen once the magnet was disassembled
- Incorporated inlet and outlet fittings along with a vacuum pump to eliminate bubbles

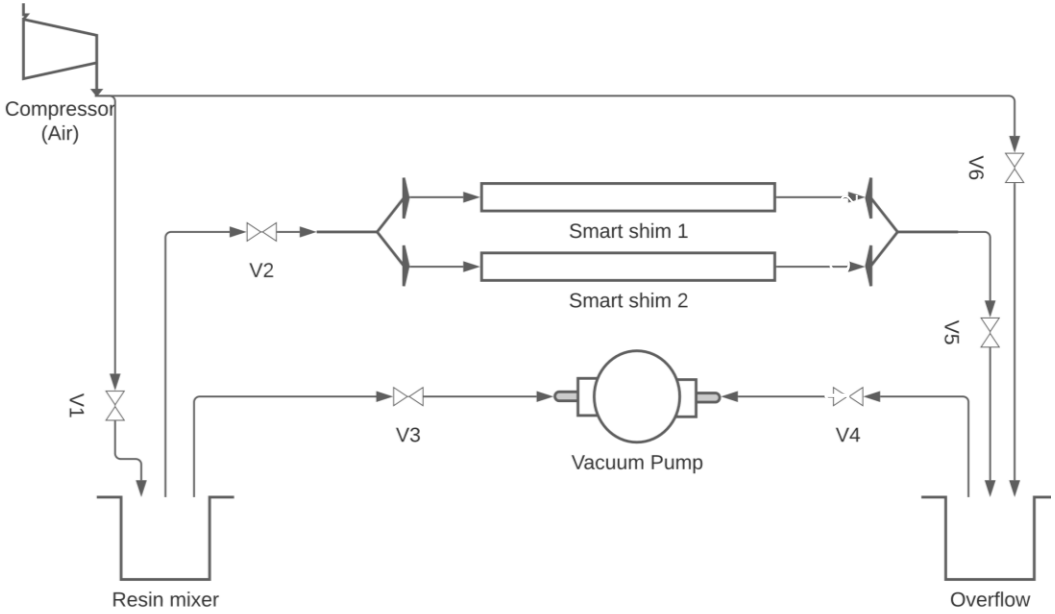

Effort led by J. L. Rudeiros, J. Swanson, M. Krutulis

Fabrication updates

Plasma coated mandrel

Visually good coverage
HiPot with bare cable failed at ~300 V

New quality control system for CCT

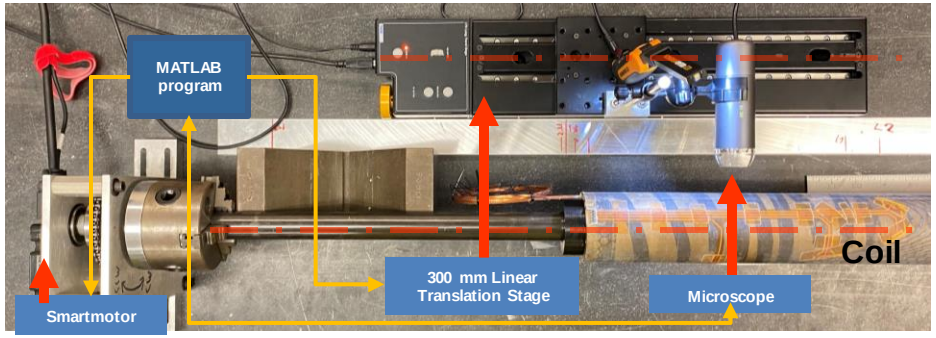

Full coil reconstruction (Image dimensions: 60803 x 19909 pixels, **1.2 Gigapixel**)

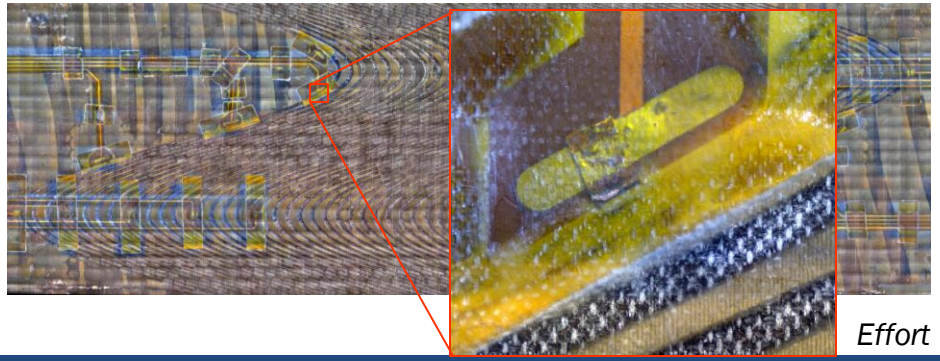

Effort led by J. L. Rudeiros

CCT Subscale 2, 3, 4 Training Summary

- **Comparison between Sub2 and sub3**
  - Subscale 3 starts at higher current quench current and trains faster initially
  - Similar training rate is seen between subscale 2 and 3 after the fast training segments with ~ 4% offset before thermal cycle
  - Some loss of memory in both magnets after thermal cycle (seems like higher loss of memory in sub3)
  - Sub3 has a higher training rate after the thermal cycle
- **Comparison between Sub2 and Sub4**
  - Sub4 starts lower than Sub2 but seems to have a higher training rate
  - Test stopped early due to higher Helium consumption than expected

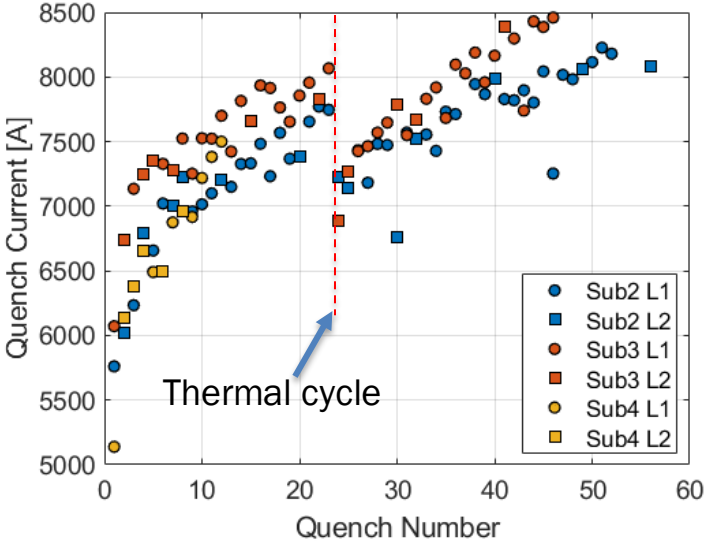

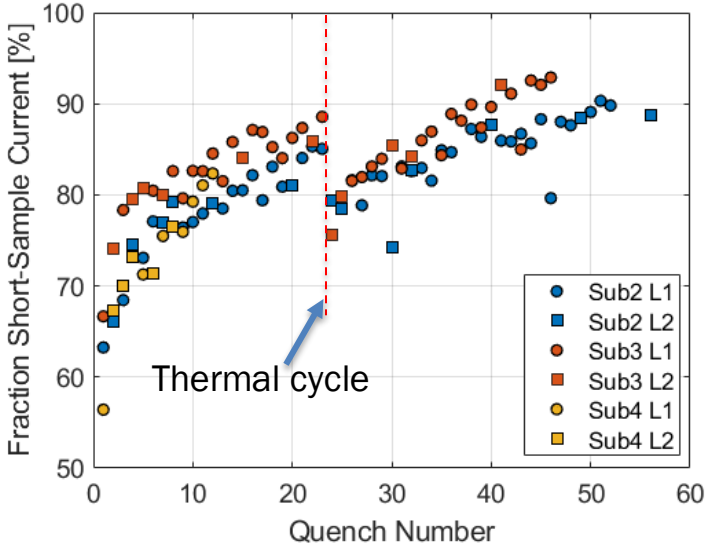

Sub2 – baseline
Sub3 – thick spar
Sub4 – CTD 701x

Latest Voltage Tap Arrangement

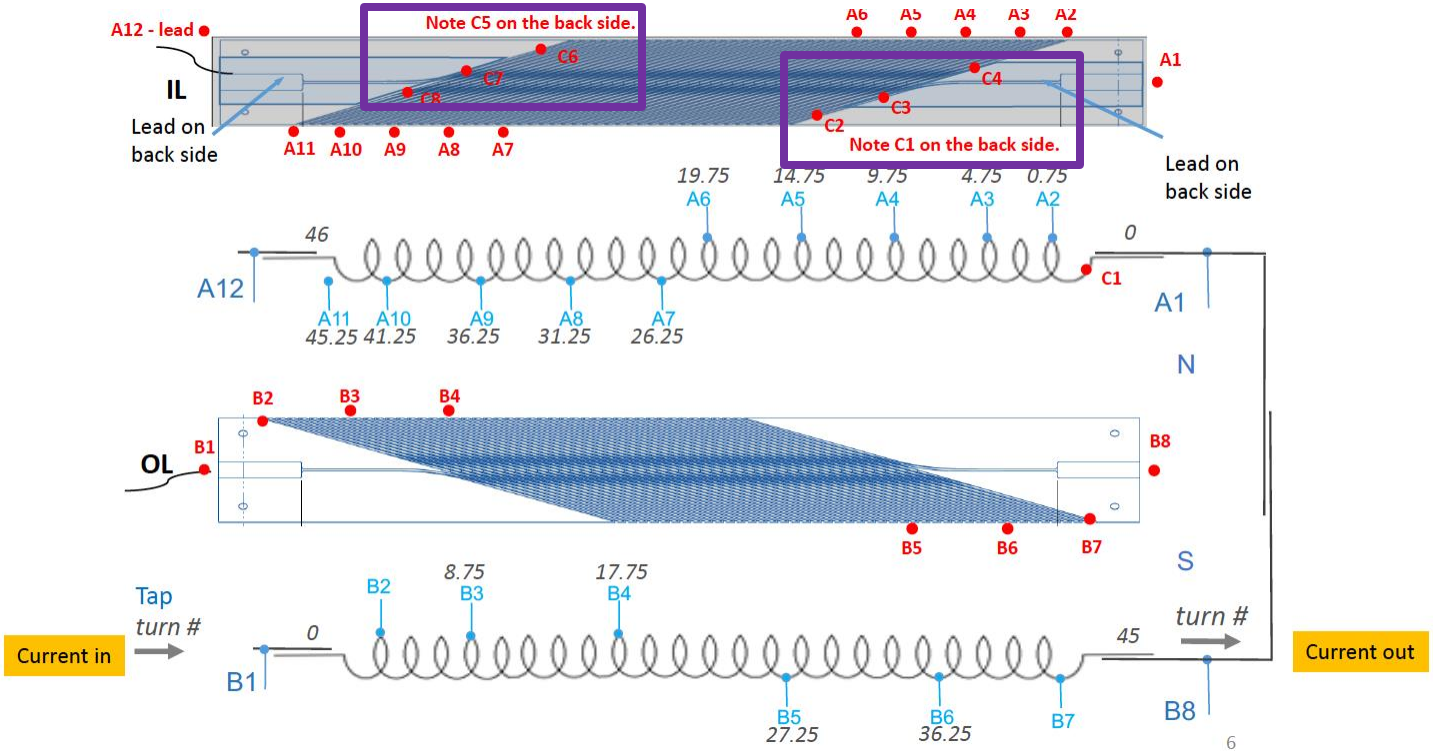

Quench Segment Distribution

Sub 2

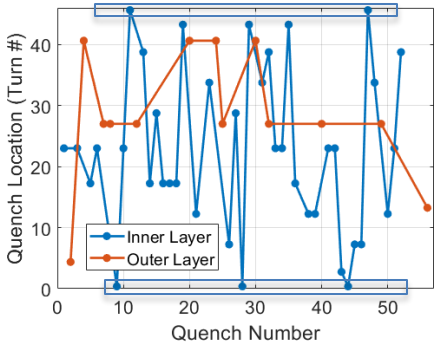

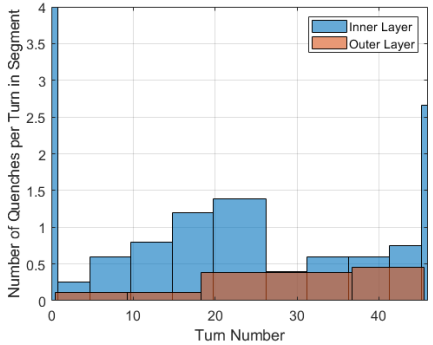

Sub 3

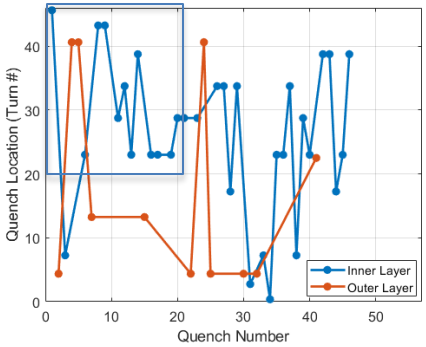

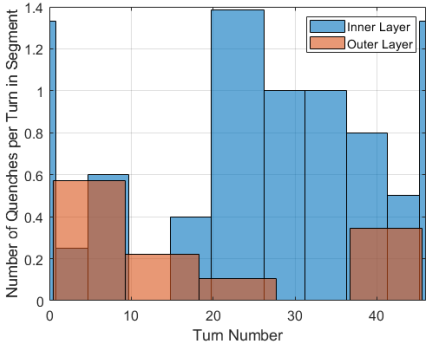

Sub 4

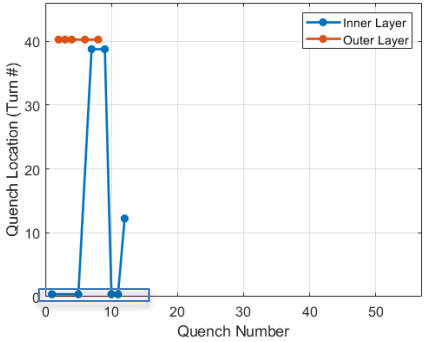

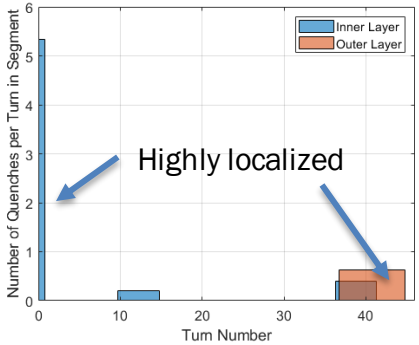

Additional Voltage Tap Data in First Turn From Each End

VT	Region monitored	Tap length (cm)
[C1, C2]	Turn 1, Pole	4.7
[C2,C3]	Turn 1, 45-degree region	6.8
[C3,C4]	Turn 1, Midplane	10.9
[C5,C6]	Turn 46, Pole	5.9
[C6,C7]	Turn 46, 45-degree region	6.7
[C7,C8]	Turn 46, Midplane	9.7

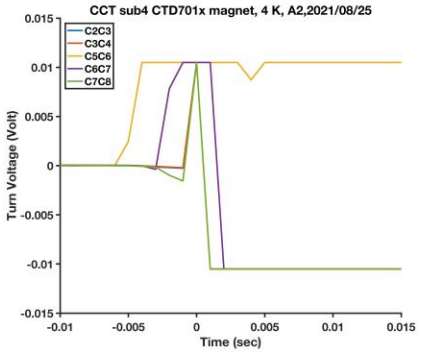

Quenches seem to originate at or near the pole region

Effort led by T. Shen

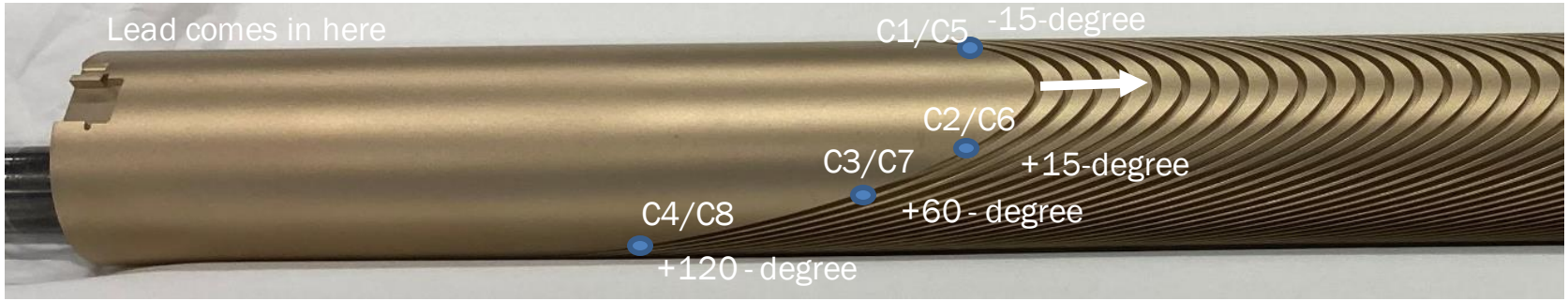

Flexible Quench Antenna

- Inter-layer antennas producing spatially resolved measurements of ramp activity and quench locations
  - Quench locations more evenly distributed in thin spar
  - Quench locations largely from 45 degrees / pole in thick spar
  - Focus has been largely experimental – detailed analysis to resume in October
- Moving forward:
  - Higher speed acquisition & increased spatial resolution
  - Simplified analytic modeling & quench heaters for validation

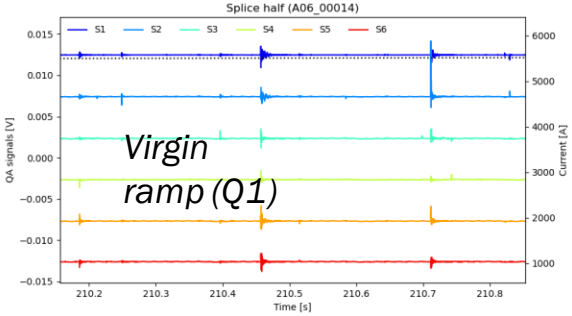

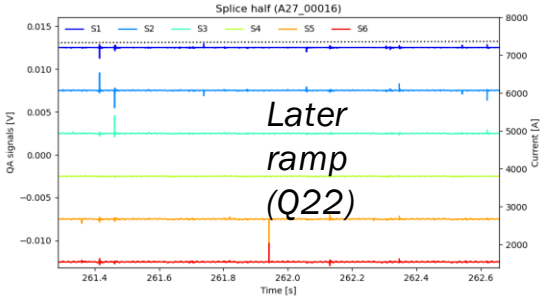

Thin spar (SUB2)

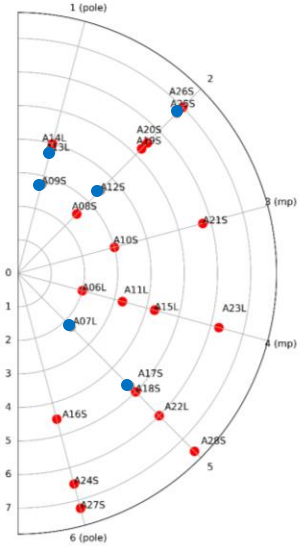

Thick spar (SUB3)

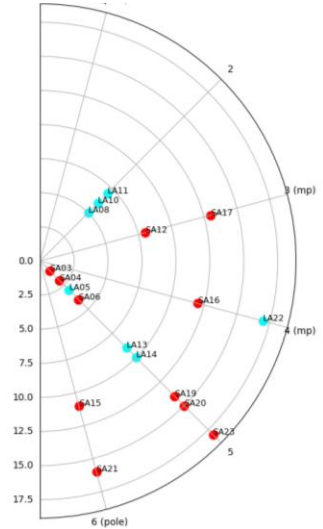

Effort led by R. Teyber, M. Marchevsky

2. Strain gauges

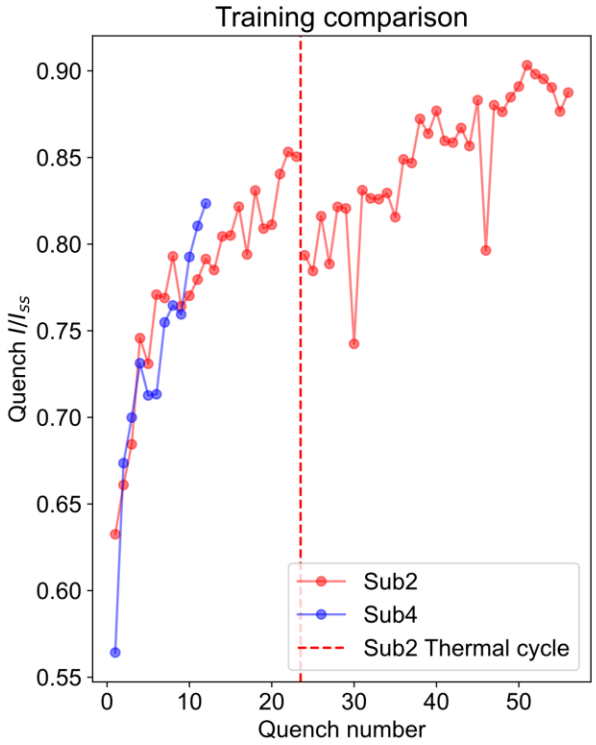

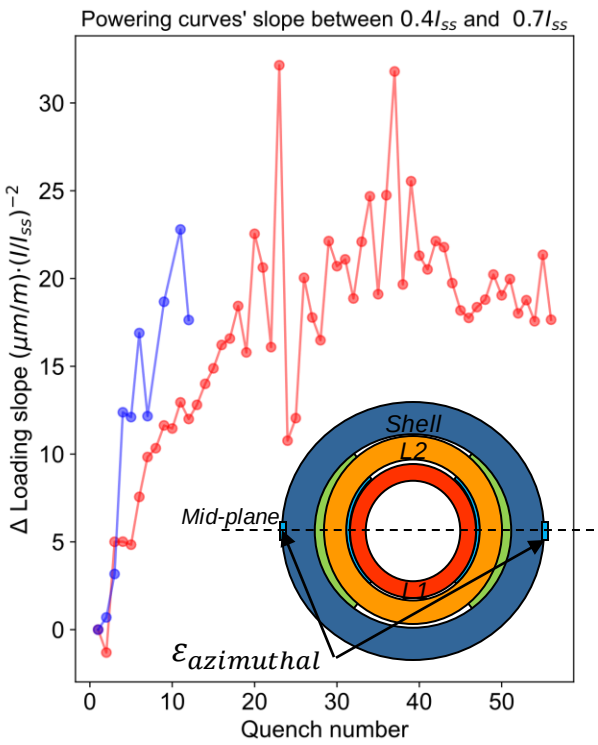

Observation

The slope of the powering curves seems to change as the training progresses.

Hypothesis

In a CCT magnet, where training might be related to interfacial mechanisms, the apparent global equivalent stiffness of the structure might change as a consequence of the accumulation of debonding events between the mandrel and the cable-epoxy system.

The global response of the structure might also change due to the relative movement between the two coils and the shell (i.e. rotation and or axial displacement). Increased alignment might lead to an apparent decrease of the global stiffness.

The slope of a $\Delta\varepsilon\ vs.\left({}^{I}/_{I_{ss}}\right)^{2}$ powering curve, as illustrated in the figure, will increase for decreasing global equivalent stiffness.

Effort led by J. L. Rudeiros

Interface Damage Model

- **Aim**: study the **differences** between the **subscale** magnets (***qualitative***). Ideally, would like to **predict/match** the behavior starting from the **measured** interfaces' properties (***quantitative***)

- **Contact** elements (bonded/frictional/**CZM**) around the cable (**cable/spar**, **cable/rib**)
  - **Bonded** model, to evaluate tension/shear loads at the interfaces
  - **Frictional** model, to evaluate potential motion with failed interfaces
  - **Cohesive** model, to model progressive failure during training

- **Elasto-plastic material** model for the **conductor**, extracted from RVE models of the cable

- **Load steps**: 0: **prestress**, 1: **cooldown**, 2: **powering** to final current

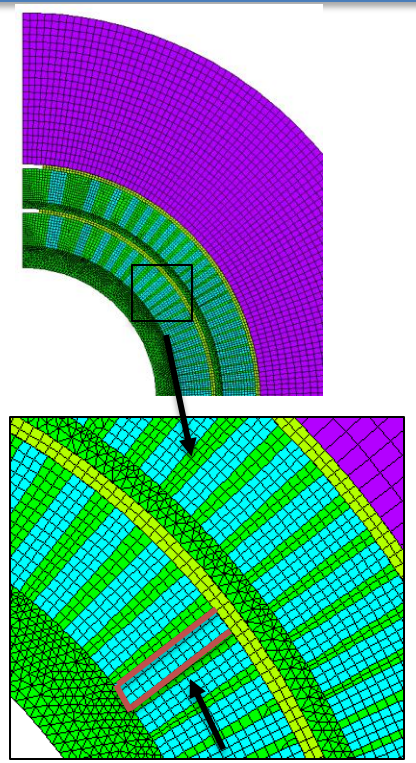

Effort led by G. Vallone

Subscale – CZM Model - Damage

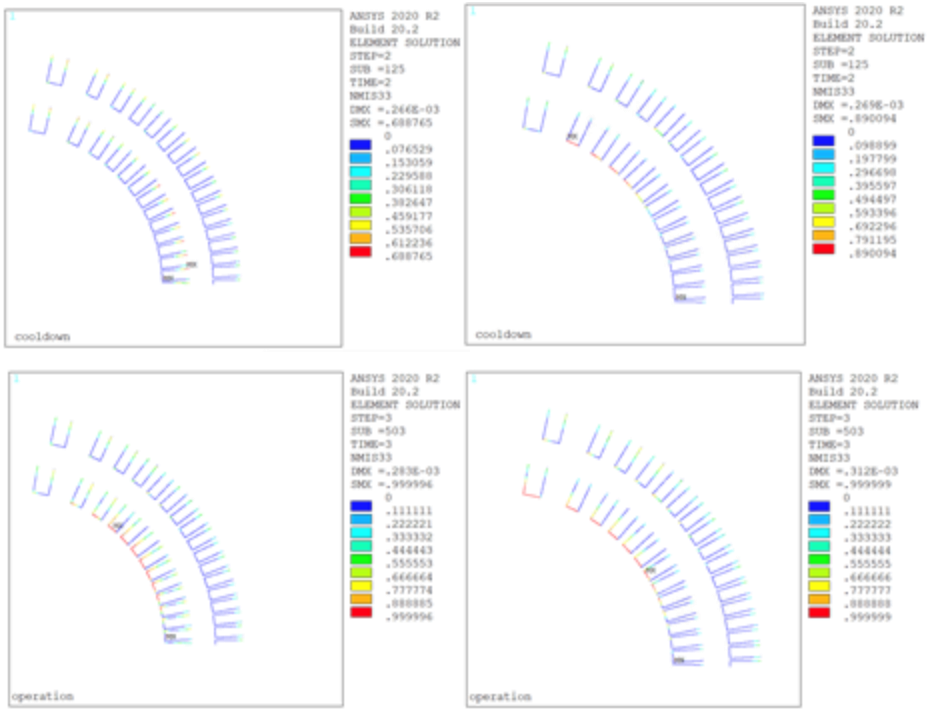

Thin Thick

N.B. Preliminary analysis, work in progress!

Damage plot: 0=undamaged, 1=completely broken

Thin spar:

- **Initial detachment** on the **outer radius** of both layers after **C.D.**
- **Full** detachment on the **spars** and **rib corners** at **45°**

Thick spar:

- **More damage** after **C.D.**
- **Different debonding locations** on the thick spar model (moved towards the pole)

→ This change in the detachment 'area' seems **coherent** with results from **AE measurements**….

Effort led by G. Vallone

3D Periodic Model for CCT6

- Compare results with the 2D model to understand where a 3D model is needed during the design
- Model the stress state of the conductor in more detail (especially at the pole region)
- Establish a more accurate model for final design optimization
- Performed sensitivity study on coil properties

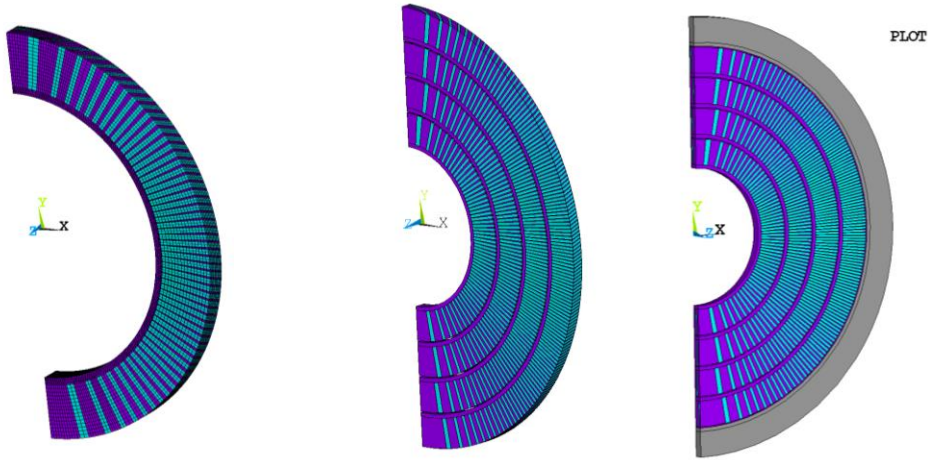

Assumes use of LD1 cable (22 x 1.4 mm)

Effort led by L. Brouwer

Sθ: Lorentz forces at 12.2 T

Isotropic (25 GPa)

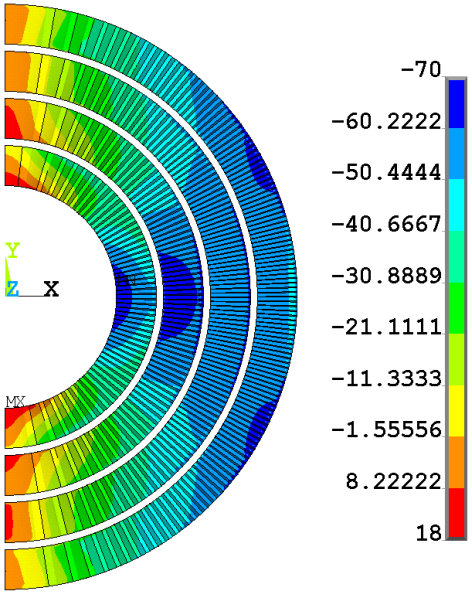

Anisotropic (elastic)

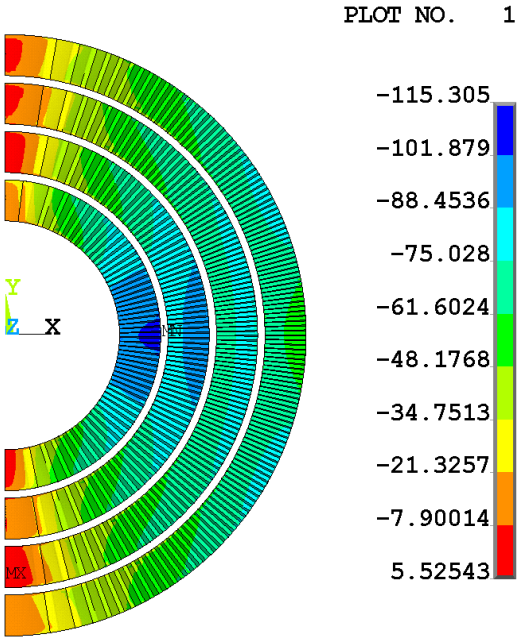

Anisotropic (elastic/plastic average)

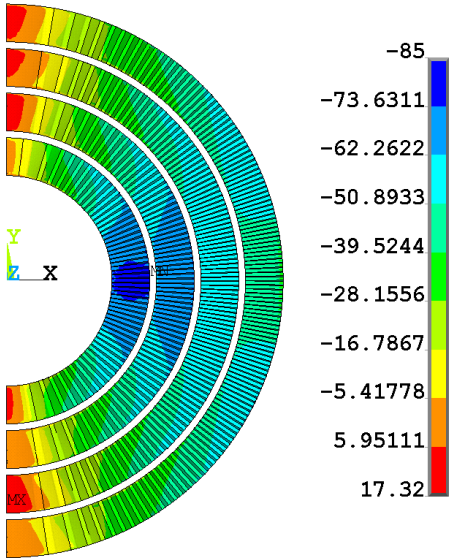

Effort led by L. Brouwer

Sz: Lorentz forces at 12.2 T

Isotropic (25 GPa)

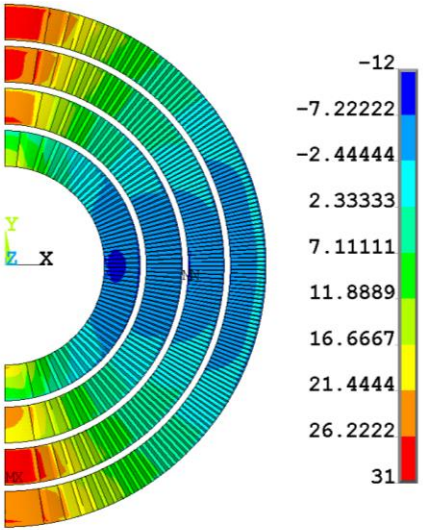

Anisotropic (elastic)

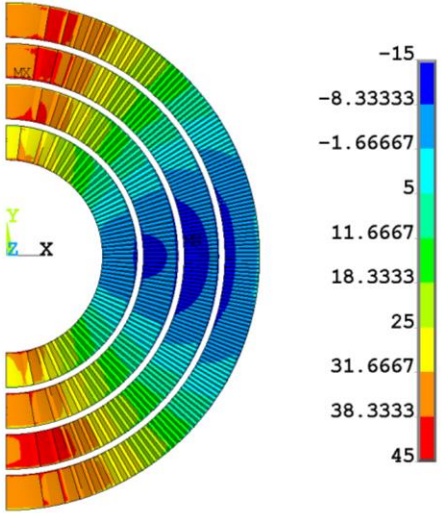

Anisotropic (elastic/plastic average)

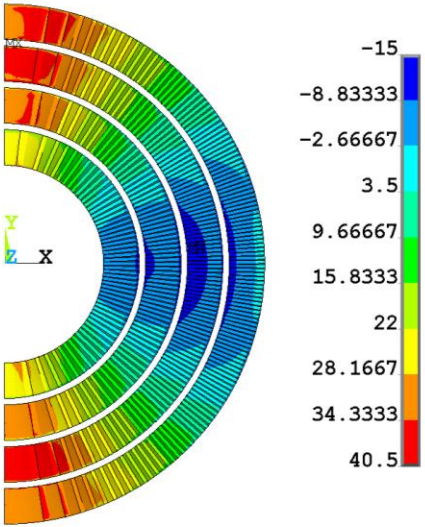

Effort led by L. Brouwer

Conclusions From Slice Model

- Stress state is reasonable (low)
- Tension at pole is expected to be somewhat artificial since de-bonding would likely occur
  - Plan to investigated non-bonded models
- Periodic (slice) 3D model agrees reasonably well with 2D analysis
  - 2D analysis is useful for the design of the structure

Current Status of CCT6 Design

Current Status

- Work on optimization of utility structure is ongoing (M. Juchno)
- Early results show that low stress in the conductor can be achieved
- Testing of deep groove machining is ongoing with good progress to date

Future Work

- Continue on utility structure optimization
- Continue to optimize deep groove machining process
- Machine 7 turn test mandrel for winding and heat treatment study

Machining Progress

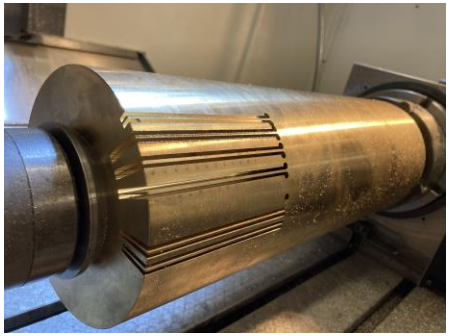

4 Layer CCT Magnet

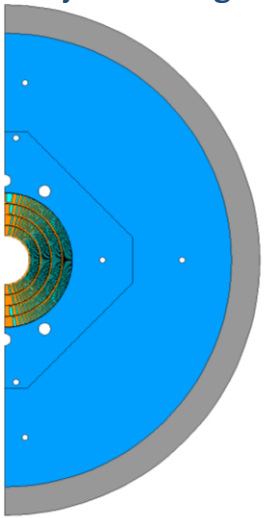

Effort led by M. Juchno, L. Brouwer, M. Maruszewski

Milestones & Deliverables for Next Fiscal Year

CCT Subscale

- Thermal cycle of sub4
- Reassembly and retest of sub2
- Wax impregnation (sub5)
- Sub6 - Possible tests: filled epoxy, High Cp material, liquid impregnation

CCT5 / hybrid

- Reassembly and retest of CCT5

CCT6

- Machining of test mandrel
- Winding and reaction of wide cable
- Layer 1 fabrication

Additional Slides

Training Summary from PSI BOX test

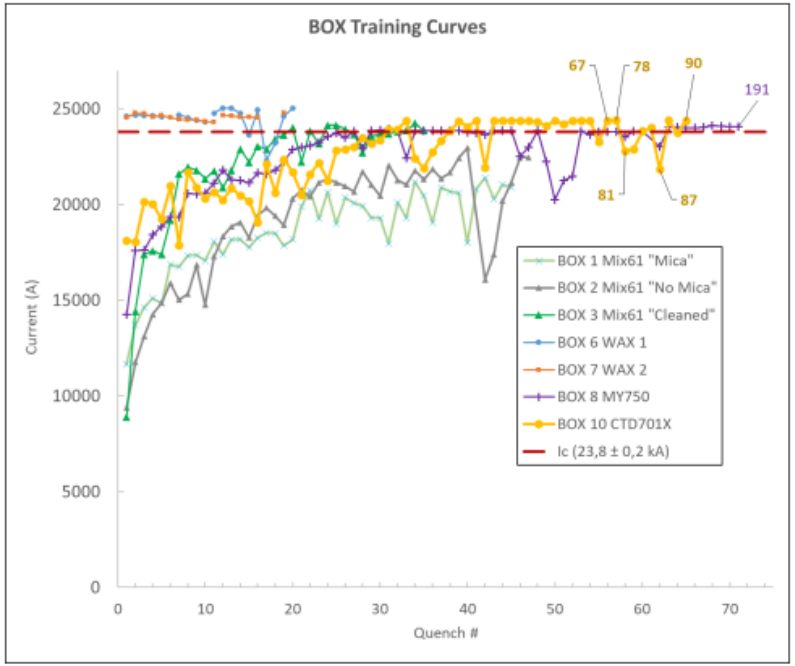

BOX Experiment Results (courtesy of M. Daly and B. Auchmann)

Resin properties – 701x has unique characteristics.

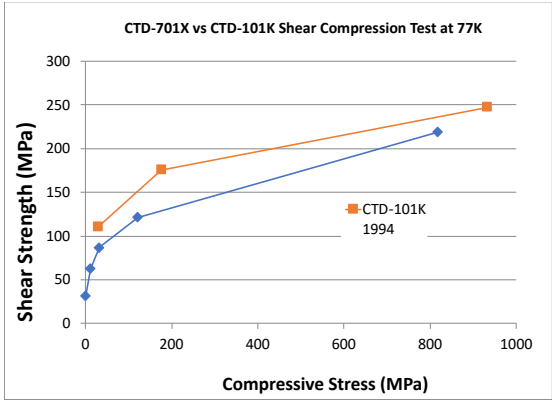

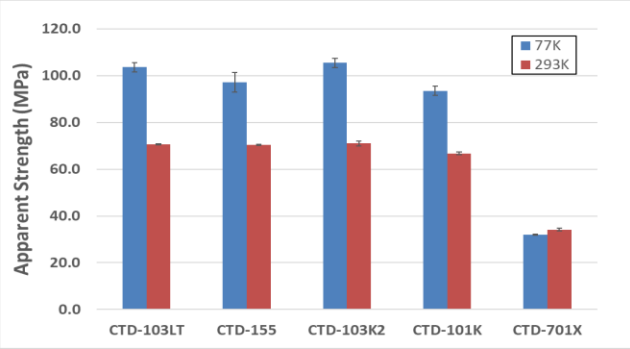

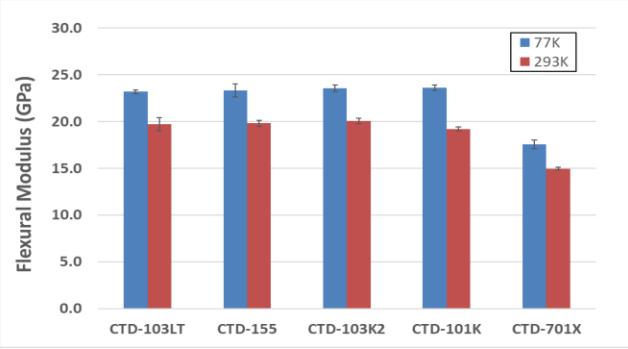

Periodic Model Assumptions

3D model properties

- conductor bonded in channel (shared mesh)
- change angle of outer layer to match pitch (more efficient)
- ~12.2 T Lorentz forces (@ 11 kA)
- conductor E = 25 Gpa
- shims are full 360 deg with 0.2 friction sliding
- rigid boundary is applied by radial displacement condition on an aluminum shell with E = 350 Gpa
- dz fit for each “layer” using iterative process (sum fz = 0)

Load steps

- cooldown + bring in rigid boundary radially
- Lorentz forces

Properties used for Sensitivity Study

From Giorgio

	Unit	R.T.		4.5 K	
		Elastic	*Plastic*	*Elastic*	*Plastic*
Ex	GPa	52.6	11.3	48	12
Ey	GPa	37.4	11.6	40.2	12.0
Ez	GPa	66.1	28.1	77.2	38.4
Gxy	GPa	18.8		17.7	
Gyz	GPa	19.9		22.5	
Gxz	GPa	22.9		24.2	
nu_xy	/	0.195	0.298	0.245	0.299
nu_zx	/	0.295	0.377	0.294	0.38
nu_zy	/	0.301	0.382	0.304	0.384
alpha_x	mm/m	4.44	4.45		
alpha_y	mm/m	4.03	4.20		
alpha_z	mm/m	3.14	3.94		

Run two anisotropic cases

1. elastic
2. average of elastic + plastic

**convert to Lucas's C.S. x->y(r), y->z(bi), z->x(tangent), xy->yz, yz->xz, xz->xy

	Elastic		Plastic		Average of Elastic-Plastic	
	293 K	4.5 K	293 K	4.5 K	293 K	4.5 K
Ex	66.1	77.2	28.1	38.4	47.1	57.8
Ey	52.6	48.0	11.3	12.0	32.0	30.0
Ez	37.4	40.2	11.6	12.0	24.5	26.1
Gxy	22.9	24.2	7.6	9.7	15.3	17.0
Gyz	18.8	17.7	4.8	4.8	11.8	11.3
Gxz	20.0	22.7	7.7	9.7	13.8	16.2
nu_xy	0.295	0.294	0.295	0.294	0.295	0.294
nu_zx	0.301	0.304	0.301	0.304	0.301	0.304
nu_zy	0.195	0.245	0.195	0.245	0.195	0.245

LD1 - Conductor and Cable Assumptions (from Paolo/GianLuca)

Parameters	Units	Pre-reaction	Post-reaction
Strand diameter	mm	0.800	0.816
Process		RRP[a]	
Stack		54/61	
Non Cu content	%	54	
Twist pitch	mm	14	
Number of strands		51	
Cable width	mm	22.00	22.36
Cable thickness	mm	1.38	1.42
Insulation thick. @ 7 MPa	μm	100	100

[a]Restacked Rod Process.

Coil Parameters

Parameter	Unit		
No. turns/quadrant (coil 1)		70	
No. turns/quadrant (coil 2)		64	
J_c at 12 T and 4.2 K	A/mm^2	3000	3300
Short sample current I_{ss} at 4.5/1.9 K	kA	16.2/18.1	16.8/18.6
Maximum bore field at 4.5/1.9 K	T	15.2/16.6	15.6/17.0
Coil peak field at I_{ss} at 4.5/1.9 K	T	16.2/17.9	16.7/18.4
Non linear stored energy at 4.5 K I_{ss}	MJ	7.4	8.0
F_x/F_y coil 1 at I_{ss} 4.5 K (1 quadrant)	MN	3.5/-0.8	3.8/-0.9
F_z coil 1 at I_{ss} at 4.5 K (1 quadrant)	MN	0.46	0.50
F_x/F_y coil 2 at I_{ss} 4.5 K (1 quadrant)	MN/m	5.6/-3.7	6.0/-4.0
F_z coil 2 at I_{ss} at 4.5 K (1 quadrant)	MN	0.74	0.80

Ref. P. Ferracin et al., IEEE TASC 22(2), 2012

strand dia.	0.8
Cu/Sc	1.2
strands	51

bw_cable	22
bw_channel	22.6
aw_cable	1.4
aw_channel	2.0

The large amount of insulation/space around the cable is the main source of inefficiently (0.3 mm on each side)